Immunity, Vol. 9, 859–869, December, 1998, Copyright ©1998 by Cell Press

TdT-Accessible Breaks Are Scattered over the Immunoglobulin V Domain in a Constitutively Hypermutating B Cell Line

Julian E. Sale and Michael S. Neuberger*
Medical Research Council Laboratory
of Molecular Biology
Hills Road
Cambridge CB2 2QH
United Kingdom

Summary

Searching for an in vitro model for somatic hypermutation, we have identified an IgM-expressing Burkitt lymphoma line that constitutively diversifies its immunoglobulin V domain at high rate during culture. As in in vivo, the mutations are largely nucleotide substitutions with the pattern of substitutions revealing a component of the human hypermutation program that is preferentially targeted to G/C residues. The substitutions frequently create stop codons with IgM-loss variants also being generated by V domain–specific deletions and duplications. However, in transfectants expressing terminal deoxynucleotidyl transferase, many IgM-loss variants additionally arise through short nontemplated nucleotide insertions into the V (but not C) domain. Thus, antibody hypermutation is likely accompanied by DNA strand breaks scattered within the mutation domain.

Introduction

The primary repertoire of antibody specificities is created by a process of DNA rearrangement involving the joining of immunoglobulin V, D, and J gene segments. Following antigen encounter in mouse and human, the rearranged V genes in those B cells that have been triggered by the antigen are subjected to a second wave of diversification, this time by somatic hypermutation. This hypermutation generates the secondary repertoire from which good binding specificities can be selected, thereby allowing affinity maturation of the humoral immune response.

Much of what we know about the hypermutation process has been derived from an analysis of the mutations that have occurred during hypermutation in vivo (for reviews see Neuberger and Milstein, 1995; Reynaud and Weill, 1996; Parham, 1998). Most of these mutations are single nucleotide substitutions that are introduced in a stepwise manner. They are scattered over the rearranged V domain, though with characteristic hotspots, and the substitutions exhibit a bias for base transitions. The mutations largely accumulate during B cell expansion in germinal centers (rather than during other stages of B cell differentiation and proliferation) with the rate of incorporation of nucleotide substitutions into the V gene during the hypermutation phase estimated at between 10^{-4} and 10^{-3} bp^{-1} generation^{-1} (McKean et al., 1984; Berek and Milstein, 1988).

The molecular mechanism of somatic hypermutation is still little understood. The possibility that lymphoid cell lines could provide a tractable system for investigating the process was considered many years ago (Coffino and Scharff, 1971; Adetugbo et al., 1977; Brüggemann et al., 1982). Clearly, it is important that the rate of V gene mutation in the cell line under study is sufficiently high not only to provide a workable assay but also to be confident that mutations are truly generated by the localized antibody hypermutation mechanism rather than reflecting a generally increased mutation rate, as is characteristically associated with many tumors. Extensive studies on mutation have been performed monitoring the reversion of stop codons in V_H in mouse pre-B and plasmacytoma cell lines (Wabl et al., 1985; Chui et al., 1995; Zhu et al., 1995; reviewed by Green et al., 1998). The alternative strategy of direct sequencing of the expressed V gene has indicated that V_H gene diversification in several follicular, Burkitt, and Hodgkin lymphomas can continue following the initial transformation event (Bahler and Levy, 1992; Jain et al., 1994; Chapman et al., 1995, 1996; Braeuninger et al., 1997). Direct sequencing has also revealed a low prevalence of mutations in a cloned follicular lymphoma line, arguing that V_H diversification can continue in vitro (Wu et al., 1995). The striking demonstration by Denépoux et al. (1997) that the BL2 Burkitt lymphoma line could be induced to undergo V_H diversification on culture with antiimmunoglobulin and activated T cells prompted us to screen other Burkitt lines for constitutive mutation. We discovered that, in Ramos, V_H mutation takes place constitutively and at high rate. This has allowed a large database of unselected mutations to be obtained, demonstrating that the V_H diversification reveals the major hallmarks of immunoglobulin gene hypermutation as deduced from in vivo studies although strongly biased to the G/C targeted phase of the mutation program. The hypermutation in Ramos leads to the frequent production of IgM-loss variants providing an assay system that can be used to obtain novel information about the hypermutation process.

Results

In order to screen for a B cell line that might undergo hypermutation in vitro, we compared the extent of diversity that had already accumulated in several human Burkitt lymphomas during previous expansion. Their rearranged V_H genes were PCR amplified from genomic DNA using multiple V_H family primers together with a J_H consensus oligonucleotide. Sequencing of the cloned PCR products revealed considerable diversity in the Ramos cell line (a prevalence of 2.8×10^{-3} mutations bp^{-1} in the V_H), although significant heterogeneity was also observed in BL41 as well as in BL2 (Figure 1A).

Mutations Have Accumulated in Ramos V_H and Vλ

We extended our analysis of V_H diversity in Ramos by sequencing the products from nine independent PCR

*To whom correspondence should be addressed (e-mail: msn@mrc-lmb.cam.ac.uk).

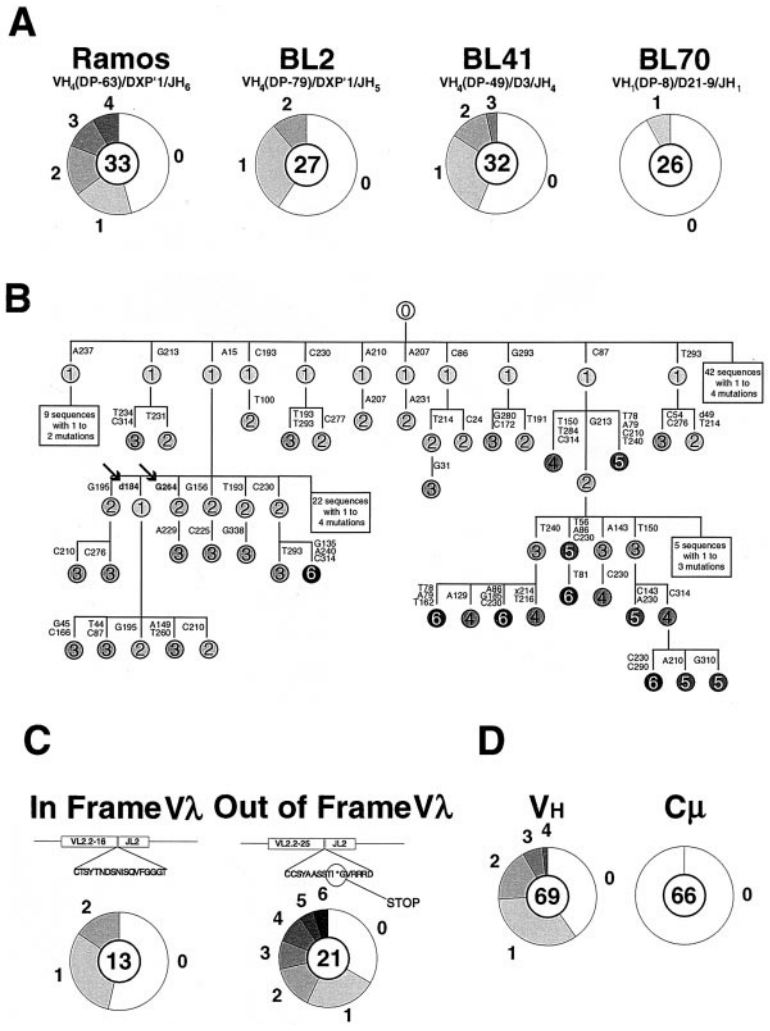

Figure 1. V_H Diversity in Burkitt Lines

(A) Sequence diversity in the rearranged V_H genes of four sporadic Burkitt lymphoma lines are shown as pie charts. The rearranged V_H genes in each cell line were PCR amplified and cloned into M13. The number of M13 clones sequenced for each cell line is denoted in the centre of the pie; the sizes of the various segments depict the proportion of sequences that are distinguished by 0, 1, 2, etc., mutations (as indicated) from the consensus. For each cell line, the consensus was taken as the sequence common to the greatest number of M13 clones and a germline counterpart (indicated above each pie) assigned on the basis of closest match using the VBASE database of human immunoglobulin sequences (Tomlinson, 1997). Our V_H consensus sequence for Ramos differs in three positions from the sequence determined by Chapman et al. (1996), five positions from that determined by Ratech (1992), and six positions from its closest germline counterpart V_H4(DP-63).

(B) Presumed dynastic relationship of V_H mutations identified in the initial Ramos culture. 315 M13V_H clones obtained from nine independent PCR amplifications were sequenced; the dynasty only includes sequences identified (rather than presumed intermediates). Each circle (with shading proportional to extent of mutation) represents a distinct sequence with the number of mutations accumulated indicated within the circle. Individual mutations are designated according to the format "C230," with 230 being the nucleotide position in the Ramos V_H (numbered as in Figure 3) and the "C" indicating the novel base at that position. The criterion used to deduce the genealogy was a minimization of the number of independent occurrences of the same nucleotide substitution. The majority of branches contain individual members contributed by distinct PCR amplifications. The rare deletions and duplications are indicated by the prefixes "x" and "d," respectively. Arrows highlight two mutations (a substitution at position 264 yielding a stop codon and a duplication at position 184) whose position within the tree implies that mutations can continue to accumulate following loss of functional heavy chain expression.

(C) Mutation prevalence in the rearranged Vλ genes. Two Vλ rearrangements were identified in Ramos. Diversity and assignment of germline origin is presented as in (A).

(D) Comparison of mutation prevalence in the V_H and Cμ regions of the initial Ramos culture. M13 clones containing cDNA inserts extending through V_H, Cμ1, and the first 87 nucleotides Cμ2 were generated by PCR from the initial Ramos culture. The pie charts (presented as in [A]) depict the extent of mutation identified in the 341 nucleotide stretch of V_H as compared to a 380 nucleotide stretch of Cμ extending from the beginning of Cμ1. The full Cμ sequence in three of the 69 M13 clones analyzed could not be unambiguously determined.

amplifications. This enabled a likely dynastic relationship between the mutated clones in the population to be deduced, minimizing the number of presumed independent repeats of individual nucleotide substitutions (Figure 1B). We are confident that PCR artefact makes little contribution to the database of mutations; not only is the prevalence of nucleotide substitutions greatly in excess of that observed in control PCR amplifications ($<0.05 \times 10^{-3}$ bp^{-1}), but we also found identically mutated clones (as well as dynastically related ones) in independent amplifications. In many cases, generations within a lineage differ by a single nucleotide substitution, indicating that only a small number of substitutions have been introduced in each round of mutation.

Analysis of Vλ rearrangements revealed that Ramos harbors an in-frame rearrangement of Vλ2.2-16 (as described by Chapman et al. [1996]) and an out-of-frame rearrangement of Vλ2.2-25. There is mutational diversity in both rearranged Vλs, although greater diversity has accumulated on the nonfunctional allele (Figure 1C).

Mutations Have Not Accumulated in Cμ

A classic feature of antibody hypermutation is that mutations largely accumulate in the V region but scarcely in the C. This is also evident in the mutations that have accumulated in the Ramos IgH locus (Figure 1D).

V_H Diversification in Ramos Is Constitutive but Is Not Associated with a General Mutator Phenotype

To address whether V gene diversification was ongoing, the cells were cloned and V_H diversity assessed using a MutS-based assay (Jolly et al., 1997) after periods of in vitro culture. The V_H gene was amplified using biotinylated

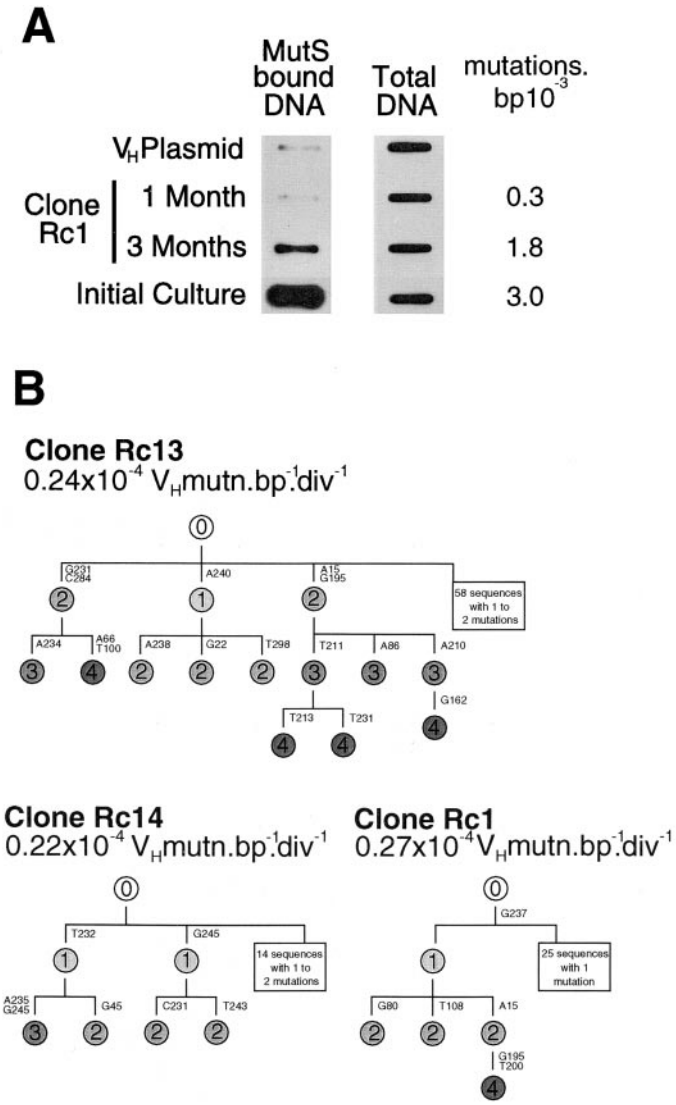

C

Clone	Rc12	Rc13	Rc14	Average
Rate of mutation to HPRT - ($\times 10^{-7}$ mutn.locus^{-1}.div^{-1})	<1.0	2.8	1.3	1.9

Figure 2. Constitutive V_H Diversification in Ramos

(A) Diversification assessed by a MutS assay. DNA was extracted from Ramos cells that had been cultured for 1 or 3 months following limit dilution cloning. The rearranged V_H was PCR amplified using biotinylated oligonucleotides prior to undergoing denaturation/renaturation; mismatched heteroduplexes were then detected by binding to immobilized MutS as previously described (Jolly et al., 1997). An aliquot of the renatured DNA was bound directly onto membranes to confirm matched DNA loading (Total DNA control). Assays performed on the Ramos V_H amplified from a bacterial plasmid template as well as from the initial Ramos culture were included for comparison. The mutation prevalence in each population as deduced by direct cloning and sequencing is indicated.

(B) V_H mutation rates in three independent clones of Ramos that had been expanded for 4 (Rc1) or 6 (Rc13 and 14) weeks, showing the dynastic relationships. Mutation rates are given per base pair per generation and were calculated by dividing the prevalence of independent V_H mutations at 4 or 6 weeks postcloning by the presumed number of cell divisions based on a generation time of 24 hr.

(C) Mutation rates at the HPRT locus were determined by fluctuation analysis. 100 cells of each clone were plated into multiple (>45) wells and allowed to expand to 3×10^6 cells prior to selection for 6-thioguanine (100 μM) resistance. Mutation rates (given per locus per generation) were calculated following the method of Luria and Delbrück (1943; Capizzi and Jameson, 1973).

oligonucleotides and, following denaturation/renaturation, mismatched heteroduplexes (arising as a consequence of mutations in V_H) were detected in a filter-binding assay using the bacterial mismatch-repair protein MutS. The results indicated that V_H diversification was indeed ongoing (Figure 2A). The V_H genes were PCR amplified from three Ramos cultures that had been expanded for 6 weeks after cloning; the sequences revealed stepwise mutation accumulation with a mutation rate of about 0.24×10^{-4} mutations bp^{-1} generation^{-1} (Figure 2B).

Direct comparison of the V_H mutation rate in Ramos to that in other cell lines is not straightforward, since there is little information on mutation rates in other lines as judged by unselected mutations incorporated throughout the V_H obtained following clonal expansion from a single precursor cell. However, the prevalence of V_H mutations following a 2 week expansion of 50 precursor BL2 cells has been determined under conditions of mutation induction (2.7×10^{-3} mutations bp^{-1}; Denépoux et al., 1997). Similar experiments performed with Ramos under conditions of normal culture reveal a V_H mutation prevalence of 2.3×10^{-3} mutations bp^{-1}. Various attempts to enhance the mutation rate by provision of cytokines, helper T cells, etc., have proved unsuccessful (data not shown). Thus, the rate of V_H mutation that can be achieved by specific induction in BL2 cells appears

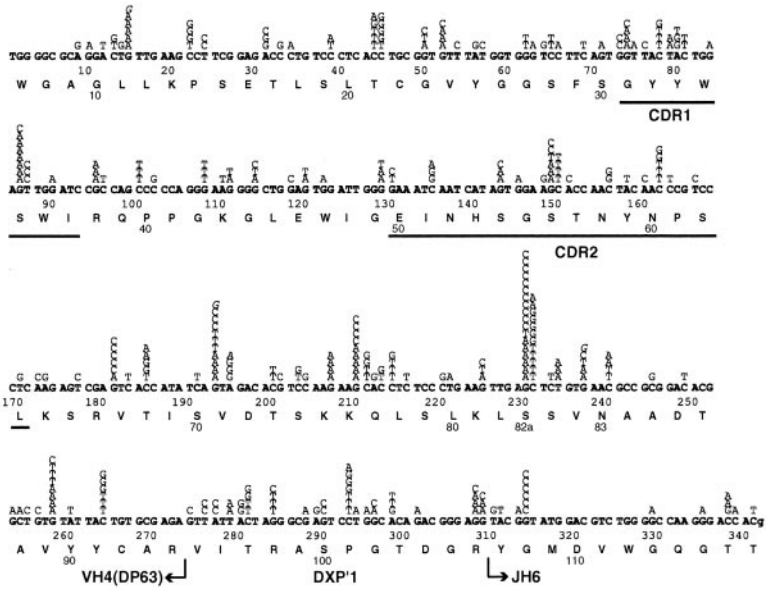

Figure 3. Distribution of Unselected Nucleotide Substitutions along the Ramos V_H

Independently occurring base substitutions are indicated at each nucleotide position. The locations of CDR1 and 2 are indicated. Nucleotide positions are numbered from the 3′-end of the sequencing primer with nucleotide position +1 corresponding to the first base of codon 7; codons are numbered according to Kabat. Mutations indicated in italics (nucleotide position 15, 193, 195, and 237) are substitutions that occurred in a mutated subclone and have reverted the sequence at that position to the indicated consensus.

to be similar to the constitutive rate of V_H mutation in Ramos.

That this high rate of mutation in V_H is not a general feature of all transcribed genes in Ramos cells is revealed by the fact that the mutation rate at the HPRT locus, as judged by fluctuation analysis of resistance to 6-thioguanine, is about 1.9×10^{-7} mutations locus^{-1} generation^{-1} (Figure 2C). This correlates well with mutation rates in other eukaryotic cell lines and, given the coding sequence length of HPRT, roughly corresponds to a mutation rate of 10^{-9} mutations base pair^{-1} generation^{-1}.

Nature of V_H Mutations in Ramos

A database of mutational events was created that combined those detected in the initial Ramos culture (from 141 distinct sequences) with those detected in four subclones that had been cultured in various experiments without specific selection (from a further 135 distinct sequences). This database was created after the individual sets of sequences had been assembled into dynastic relationships (as detailed in the legend to Figure 1B) to ensure that clonal expansion of an individual mutated cell did not lead to a specific mutational event being counted multiple times. Here, we describe an analysis of this composite database of 340 distinct and presumably unselected mutational events (200 contributed by the initial Ramos culture and 140 from the expanded subclones); separate analysis of the initial and subclone populations yielded identical conclusions.

The overwhelming majority of the mutations (333 out of 340) are single nucleotide substitutions. A small number of deletions (four) and duplications (three) but no untemplated insertions were observed; these events are further discussed below. There were only five sequences that exhibited nucleotide substitutions in adjacent positions; however, in three of these five cases, the genealogy revealed that the adjacent substitutions had been sequentially incorporated. Thus, the simultaneous creation of nucleotide substitutions in adjacent positions is a rare event.

The distribution of the mutations along the V_H is highly nonrandom (Figure 3). The major hotspot is at the G and C nucleotides of the Ser82a codon, which has previously been identified as a major intrinsic mutational hotspot in other V_H genes (Wagner et al., 1995; Jolly et al., 1996) and conforms to the RGYW consensus (Rogozin and Kolchanov, 1992; Betz et al., 1993). (While the dominant intrinsic mutational hotpot in many V_H genes is at Ser31, this codon is not present in the Ramos consensus V_H [or its germline counterpart], which have Gly at that position.) The individual nucleotide substitutions show a marked bias in favor of transitions (51% rather than randomly expected 33%). There is also a striking preference for targeting G and C that account for 82% of the nucleotides targeted (Table 1); this is considered in the Discussion.

Hypermutation Generates Diverse IgM-Loss Variants

Analysis of the Ramos variants revealed several mutations that must have inactivated V_H (see legend to Figure 1B), suggesting it might be possible for the cells to lose IgM expression but remain viable. Analysis of our original Ramos culture revealed it to contain 8% surface IgM$^-$ cells. Such IgM-loss variants can be generated during in vitro culture: flow cytometric analysis of two

Table 1. Nucleotide Substitution Preferences of Hypermutation in Ramos

	Frequency of Substitution to				
Parental Nucleotide	T	C	G	A	Total
T	—	3.9	1.2	3.0	8.1
C	17.4	—	12.6	4.8	34.8
G	7.2	15.9	—	24.0	47.1
A	2.4	1.8	5.7	—	9.9

Single nucleotide substitutions were computed on the V_H coding strand and are given as the percentage of the total number (333) of independent, unselected nucleotide substitutions identified.

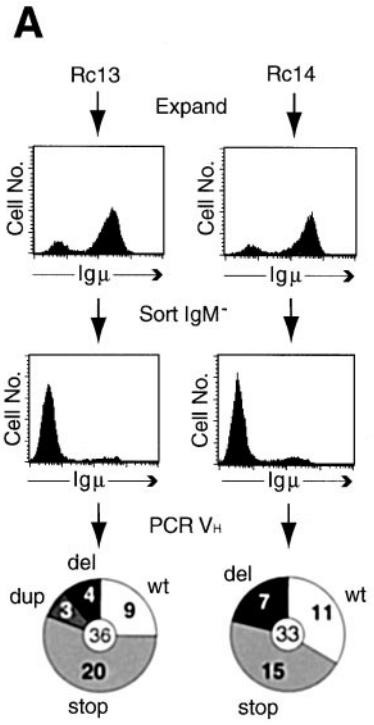

Figure 4. Hypermutation in Ramos Generates Diverse Revertible IgM-Loss Variants

(A) Scheme showing the isolation of IgM-loss variants. The starting Ramos culture was transfected with pSV2neo, diluted into 96-well plates, and clones growing in selective medium were allowed to expand. Flow cytometry performed on the expanded clones 6 months after the original transfection revealed the presence of IgM-loss variants, constituting 16% and 18% of the two clonal populations (Rc13 and Rc14) shown here. Enrichment by a single round of sorting yielded subpopulations that contained 87% (Rc13) and 76% (Rc14) surface IgM-negative cells. Following PCR amplification of the rearranged V_H gene in these subpopulations, sequencing revealed that 75% (Rc13) and 67% (Rc14) of the cloned V_H segments contained a nonsense (stop), deletion (del), or duplication (dup) mutation within the 341 nucleotide V_H stretch analyzed. The remainder of the clones were designated wild-type (wt) although no attempt was made to discriminate possible V_H-inactivating missense mutations. The four deletions and three duplications identified in the Rc13 population are all distinct, whereas only four distinct mutations account for the 7 Rc14 sequences determined that harbor deletions. The nature of the deletions and duplications is presented in Figure 6.

(B) Multiple nonsense mutations can contribute to V_H inactivation. The panel summarizes the nature of the stop codons observed in the Rc13 and Rc14 IgM-loss populations. Each V_H codon position at which stops were observed in these two populations is listed. Thus, at least eight independent mutational events yielded the nonsense mutations that account for 20 out of the 27 nonfunctional V_H sequences in the Rc13 database; a minimum of ten independent mutational events yielded the nonsense mutations that account for 15 of the 22 nonfunctional V_H sequences in the Rc14 database. The numbers in parentheses after each stop codon give the number of sequences in that database that carry the relevant stop codon followed by the number of these sequences that are distinct, as discriminated on the basis of additional mutations. Analysis of stop codons in IgM-loss variants selected from four other clonal populations (data not shown) revealed stop codon creation at a further five locations within V_H.

(C) Reversion of IgM-loss variants. IgM-loss variants sorted from Rc13 were cloned by limiting dilution. Three weeks after cloning, the presence of IgM^+ revertants in the IgM^- subclones was screened by cytoplasmic immunofluorescence analysis of 5×10^4 cells; their prevalence is given. These IgM^+ revertants were then enriched in a single round of sorting and the V_H sequences of the clonal IgM^- variant compared to that it of its IgM^+ revertant descendants.

(D) The sequence surrounding the stop codons in the IgM-loss derivatives of Rc13 reveals that TAG32 conforms well to the RGYW consensus (R, purine; Y, pyrimidine; and W, A or T; Rogozin and Kolchanov, 1992), which accounts for a large proportion of intrinsic mutational hotspots (Betz et al., 1993), whereas TAA33 and TGA36 do not.

surface IgM^+ Ramos subclones that had been cultured in vitro for 6 months revealed 16% and 18% IgM^- cells (Figure 4A). These IgM^- cells were enriched in a single round of sorting prior to PCR amplification and cloning of their V_H segments. The sequences revealed a considerable range of V_H-inactivating mutations (stop codons or frameshifts) (Figure 4), although diverse inactivating mutations were even evident in IgM-loss variants sorted after only 6 weeks of clonal expansion (see Figure 5).

The stop codons were created at a variety of positions (Figure 4B) but were not randomly located. In data obtained in six independent experiments, stop codon creation was restricted to 16 of the 39 possible sites; the DNA sequences at these preferred sites being biased (on either coding or noncoding strand) toward the RGYW consensus (data not shown).

Not surprisingly, whereas deletions and insertions account for only a small proportion of the mutations in unselected Ramos cultures (see above), they make a much greater contribution when attention is focused on V_H-inactivating mutations. It is notable that a large proportion of the IgM-loss variants can be accounted for by stop-codon/frameshift mutations in the V_H itself. This further supports the proposal that hypermutation in Ramos is preferentially targeted to the immunoglobulin V domain—certainly rather than the C domain or, indeed, other genes (such as the Igα/Igβ sheath) whose mutation could lead to a surface IgM^- phenotype. It also may well be that the Ramos V_H is more frequently targeted for hypermutation than its productively rearranged Vλ, a conclusion supported by the pattern of mutations in the initial culture (Figure 1C).

Reversion of IgM-Loss Variants

The dynasty established earlier (Figure 1B) suggested not only that IgM^- cells could arise but also that they might undergo further mutation. To confirm this, the cells in the sorted IgM^- population were cloned and allowed to expand for 3 weeks. Cytoplasmic immunofluorescence of ten expanded clonal populations revealed the presence of IgM^+ revertants at varying prevalence (from 0.005% to 1.2%; Figure 4C), allowing a mutation

rate of 1×10^{-4} mutations bp^{-1} $generation^{-1}$ to be calculated by fluctuation analysis. This is somewhat greater than the rate calculated by direct analysis of unselected mutations (0.25×10^{-4} mutations bp^{-1} $generation^{-1}$; see above), probably in part reflecting that different IgM-loss clones revert at different rates depending upon the nature of the disrupting mutation. Indeed, sequence analysis of the V_H in four of the IgM^- clones (and their descendants) revealed that the two that gave rise to a high frequency of revertants harbored a stop codon that lay within a mutational RGYW hotspot consensus; the two low frequency revertants harbored stop codons that did not (Figure 4D).

Nucleotide Insertions into V_H in TdT Transfectants

The availability of cell lines that constitutively diversify their V gene segments should facilitate investigations into the mechanism of hypermutation. Thus, for example, although somatic hypermutation, IgH class-switching, and RAG-mediated joining can all occur in germinal center B cells, results with the Ramos line indicate that the processes are not intimately linked. We have not detected any class-switching in Ramos (<1 in 10^5 cells are IgG^+ [even among the sorted IgM^- population] as judged by cytoplasmic immunofluorescence). Similarly, although spliced RAG1 and RAG2 mRNAs were detectable in the initial Ramos culture by RT-PCR at an abundance some 100-fold less than in a human pre-B lymphoma line (Nalm6), the levels varied among Ramos subclones with RAG1 mRNA being undetectable in one of the mutating subclones. That hypermutation can therefore presumably occur independently of RAG1 is consistent with the findings of Zheng et al. (1998).

If the mechanism of hypermutation involves a DNA polymerase (rather than being achieved exclusively, for example, by base-modifying enzymes that do not cleave the sugar-phosphate backbone), then it is likely accompanied by strand breaks, since DNA polymerases extend on free 3′-hydroxyl groups. The breaks could be single- or double-stranded and occur at multiple or scattered sites either within or adjacent to the immunoglobulin V region. LM-PCR has been used to screen for breaks in the IgH locus in germinal center B cells (Lo et al., 1997), but without such breaks being present at high frequency or having a specific sequence signature, it has not been possible to conclude that the breaks detected were not simply created during DNA extraction or due to apoptotic cells. We have performed LM-PCR on DNA gently extracted from Ramos but have not so far seen evidence of an increased abundance of flush-end double-strand breaks in the V_H as opposed to C_H region. We therefore adopted a distinct approach to screening for DNA breaks, exploiting the activity of terminal deoxynucleotidyl transferase (TdT) to add nontemplated nucleotides to DNA ends. If DNA breaks were occurring in the V_H segment during antibody hypermutation, then TdT-catalyzed nucleotide insertion could contribute significantly to the creation of IgM-loss variants.

A plasmid encoding TdT under control of the β-globin promoter and IgH intronic-enhancer was transfected into Ramos and expression in three independent clones confirmed by Western blotting (Figure 5A). Greater than

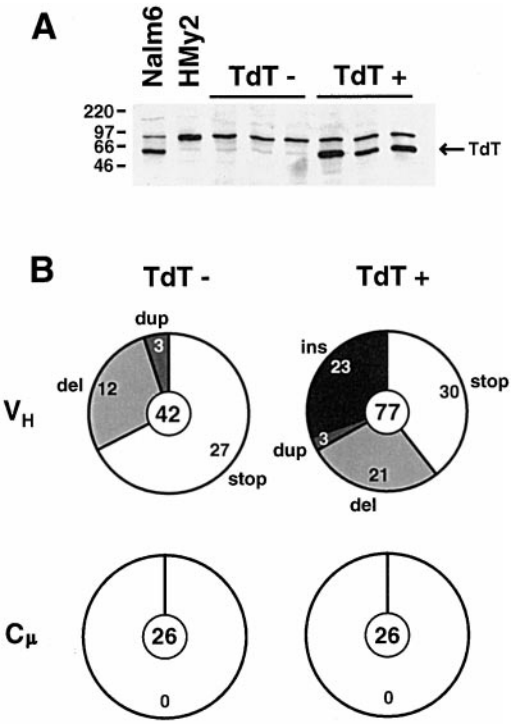

Figure 5. IgM-Loss Variants in Ramos Transfectants Expressing TdT

(A) Expression of TdT in three pSV-pβG/TdT and three control transfectants of Ramos was compared by Western blot analysis of nuclear protein extracts; control transfectants were obtained using a pSV2neo plasmid that did not contain the TdT gene. (Nalm6 is a TdT-positive human pre-B cell lymphoma and HMy2 is a TdT-negative mature human B cell lymphoma).

(B) Pie charts depicting independent mutational events giving rise to IgM-loss variants. IgM^- variants (constituting 1%–5% of the population) were obtained by sorting the three TdT^+ and three TdT^- control transfectants that had been cultured for 6 weeks following cloning. The V_H regions in the sorted subpopulations were PCR amplified and sequenced. The pie charts depict the types of mutation giving rise to V_H inactivation with the data obtained from the TdT^+ and TdT^- IgM^- subpopulations separately pooled. Abbreviations are as in Figure 4A except that "ins" indicates clones containing apparently nontemplated nucleotide insertions. Clones containing deletions or duplications together with multiple nucleotide nontemplated insertions are only included within the "ins" segment of the pie. Only unambiguously distinct mutational events are computed. Thus, of the 77 distinct V_H-inactivating mutations identified in the TdT^+ IgM-loss subpopulations, 30 distinct stop codon mutations were identified; if the same stop codon had been independently created within the IgM-loss population derived from a single Ramos transfectant, this would have been underscored. As indicated by the pies, none of the Cμ sequences from the IgM^- cells revealed mutations.

90% of the cells in each of these three transfectants revealed nuclear TdT as judged by immunofluorescence (data not shown). After culturing for 6 weeks post-transfection, IgM^- subpopulations were obtained in a single round of cell sorting. Their rearranged V_H segments were PCR amplified, cloned, and sequenced. In total, 77 distinct nonfunctional V_H sequences were obtained from the TdT^+ transfectants. For comparison, the V_H genes were amplified from the surface IgM^- variants obtained from three TdT-negative control transfectants, yielding 42 nonfunctional sequences. The mutations

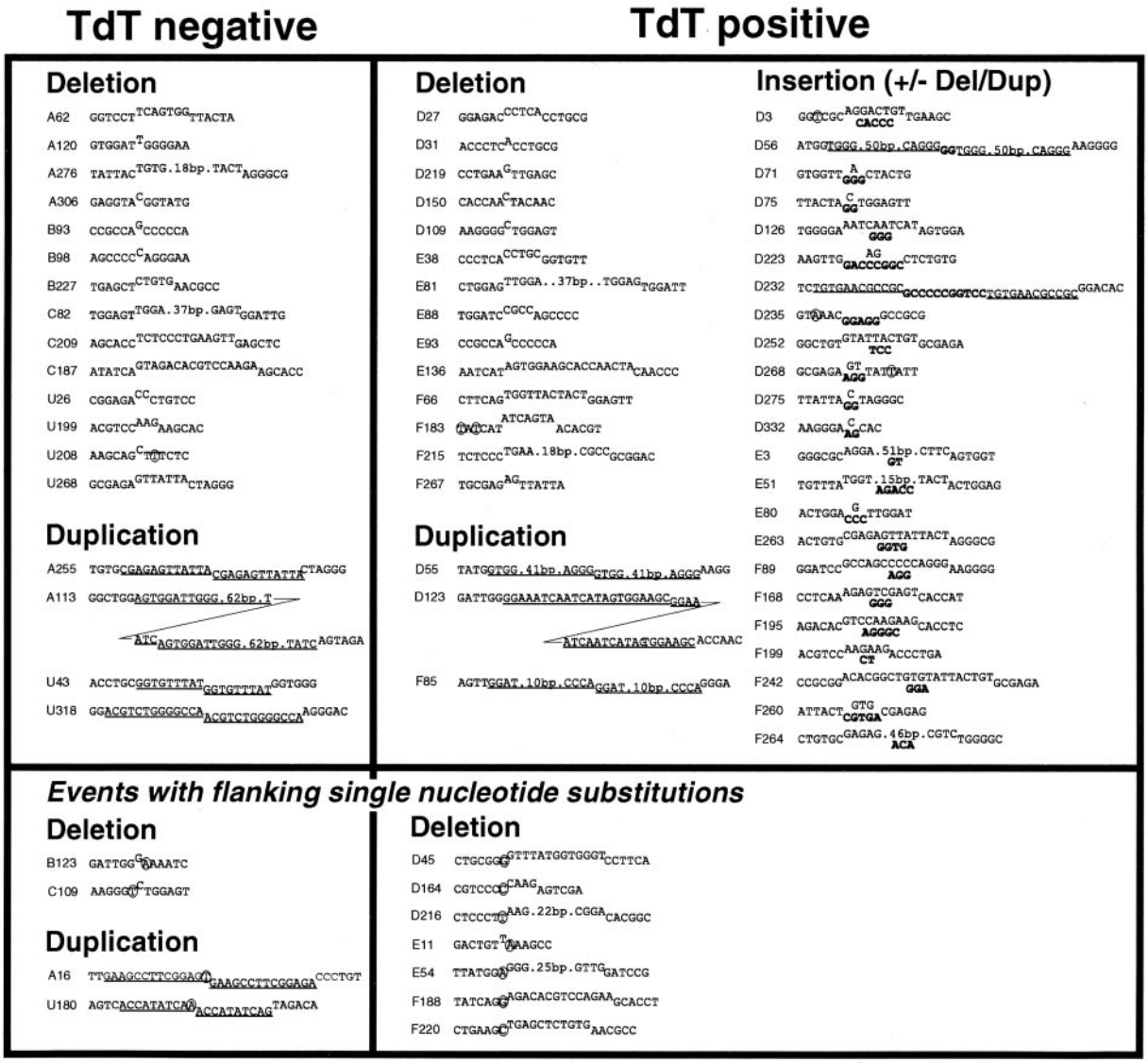

Figure 6. Mutations in V_H Other Than Single Nucleotide Substitutions

Each event is named with a letter followed by a number. The letter gives the provenance of the mutation (A, B, and C being the cloned TdT$^-$ control transfectants, D, E, and F the TdT$^+$ transfectants, and U signifies events identified in the initial, unselected Ramos culture; the transfectants in group C, D, E, and F were grown for 6 weeks prior to sorting of the IgM$^-$ population, whereas A and B were grown for 6 months); the number indicates the first nucleotide position in the sequence string. Nucleotides deleted are specified above the line and nucleotides added (duplications or nontemplated insertions) below the line; single nucleotide substitutions are encircled with the novel base being specified. The duplicated segments of V_H origin are underlined; nontemplated insertions are in bold. With several deletions or duplications, the event is flanked by a single nucleotide of unknown provenance. Such flanking changes could well arise by nucleotide substitution (rather than nontemplated insertion) and these events therefore are separately grouped; the assignment of the single base substitution (encircled) to one or other end of the deletion/duplication is often arbitrary.

rendering the V_H nonfunctional were grouped into nucleotide substitutions (stops), deletions, duplications, and nontemplated insertions.

The grouping of the V_H sequences obtained from the TdT$^-$ control transfectants was straightforward. The majority of the inactivating mutations could be ascribed to stop codons (27 examples) with the remainder (15 examples) being due to deletions or tandem duplications, of which three were accompanied by a single flanking nucleotide substitution (Figures 5B and 6). These categories of mutation were detected in our initial Ramos culture and have also been identified in other studies (see Goosens et al., 1998; Wilson et al., 1998). No example of a mutation that was likely due to nontemplated insertion was identified either among the TdT$^-$ clones or in the initial Ramos culture.

In contrast, only 54 of the 77 nonfunctional V_H sequences from the TdT$^+$ transfectants could be accounted for by stop codons (30 examples), simple deletions (14), simple duplications (3), or deletions with a single flanking nucleotide substitution (7). The remaining 23 sequences all carry the hallmarks of nontemplated

nucleotide insertions. One cannot be 100% unequivocal that these insertions are all untemplated since, given their short length, a possible donor sequence will likely exist either within the V gene or elsewhere in the human genome; apparently nontemplated insertions could also be created by a complex patchwork of microduplications and deletions. However, we regard it as unlikely that such explanations could account for more than a small proportion of the putative nontemplated insertions. The apparent insertions are found in multiple examples (4, 7, and 12) in each of the three TdT^+ transfectants; they are not observed in any of the TdT^- controls or in the V_H database from unselected Ramos cells. The insertions show the typical hallmarks of being catalyzed by TdT as judged by the paradigm of N region insertions at V(D)J junctions (Alt and Baltimore, 1982): they are short (2–11 nucleotides) and they are G/C rich (G+C account for 79% of the inserted bases). It is notable that all but one of the insertions are accompanied by short deletions or duplications; such events are likely consequences of the rejoining of a DNA molecule that contains a tailed 3-hydroxyl. The nontemplated insertions appear peculiar to the hypermutation domain, since we did not detect such insertions (or indeed any other mutation) in the Cμ1/2 domains sequenced from 26 PCR-amplified genomic Cμ clones generated from the IgM^- population (Figure 5B). Indeed, the presence of TdT had no significant effect on the global mutation rate in Ramos; fluctuation analysis of 6-thioguanine resistance indicated a mutation rate at the HPRT locus of 2.6×10^{-7} mutations $locus^{-1}$ $generation^{-1}$ in the TdT transfected cells compared with 1.9×10^{-7} mutations $locus^{-1}$ $generation^{-1}$ in the parental cell line (see Figure 2C).

The published literature provides a large database of V gene mutations generated by somatic hypermutation. Since most mature human B cells lack TdT, one would predict that nontemplated insertions would not feature as a major contributor to that database. This is indeed the case. Deletions and insertions have certainly been identified in other studies (Wu and Kaartinen, 1995; Goosens et al., 1998; Wilson et al., 1998), but nearly all the insertions have been attributed to simple tandem duplications (possibly with a single flanking nucleotide substitution) or can be retrospectively so identified (e.g., Ann36 in Goosens et al., 1998). Indeed, the only examples of insertions that are not duplications that we have been able to trace are a possible 35 nucleotide insertion with 20 nucleotide identity to the Bacillus cereus *pur9* gene obtained following single cell PCR from tonsil (Goosens et al., 1998) and up to five examples of single nucleotide insertions (Kim et al., 1981; Kosmas et al., 1996; Frey et al., 1998; Goosens et al., 1998; Wilson et al., 1998). Single nucleotide insertions have frequently been found at the sites of blunt-end joining in TdT-negative cells with the demonstrated ability of DNA polymerases to add single nucleotides to the ends of blunt duplexes being invoked to explain their genesis (Clark, 1988; Phillips and Morgan, 1994). In any case, the short, nonduplicative >1 nucleotide insertions characteristic of the mutations in the TdT-expressing Ramos transfectants have no counterpart in either the control Ramos transfectants or in the published database of V gene mutations.

Discussion

The Ramos Burkitt line constitutively diversifies its rearranged immunoglobulin V gene during in vitro culture. This hypermutation does not require stimulation by activated T cells, exogenously added cytokines, or even maintenance of the B cell antigen receptor.

The rate of V_H mutation (which lies in the range $0.2–1 \times 10^{-4}$ bp^{-1} $generation^{-1}$) is at least four orders of magnitude higher than that observed at the HPRT locus. It is sufficiently high to readily allow the accumulation of a large database of unselected mutations and so reveal that hypermutation in Ramos exhibits most of the features classically associated with immunoglobulin V gene hypermutation in vivo (preferential targeting of mutation to the V as opposed to C or other genes within the cell, stepwise accumulation of single nucleotide substitutions, transition bias, and characteristic mutational hotspots). The large majority of mutations in the unselected database are single nucleotide substitutions, although deletions and duplications (sometimes with a flanking nucleotide substitution) are detectable. Such deletions and duplications have also been proposed to be generated as a consequence of hypermutation in vivo (Wu and Kaartinen, 1995; Goosens et al., 1998; Wilson et al., 1998).

G/C-Biased Phase of V Gene Hypermutation

A feature of V_H diversification in Ramos that differs from somatic hypermutation as characterized in mice is the preferential targeting of G and C nucleotides: 82% of all the unselected nucleotide substitutions in the Ramos V_H were at G/C residues (Table 1) compared to corresponding figures in the range 47%–54% for unselected mutations generated in mouse V genes in vivo, where A is the most commonly mutated base (Milstein et al., 1998).

Various explanations can be envisaged for this discrepancy. It could be a consequence of the difference in the DNA substrates analyzed. Since hypermutation is not targeted randomly, an increased abundance of G/C-rich hotspot motifs in the DNA target could lead to an increased G/C bias in the overall mutation pattern. However, even if the four major mutational hotspots are removed from the analysis of Ramos V_H mutation, a G/C targeting of 79% is still evident. Alternatively, the nucleotide targeting of hypermutation in humans could differ from that in mouse. However, while there are few data on unselected V gene mutations in human, G/C mutations accounted for only 62% of the total of 1307 mutations in the V_H26 gene in human memory B cells (Wagner et al., 1996).

Thus, the preferential targeting of G/C nucleotides appears to reflect a major distinction between hypermutation in Ramos and the process that occurs in vivo. This favors the idea that part of the hypermutation program in normal human germinal center B cells is G/C biased (this being the phase that takes place in Ramos) but that additional processes also occur in vivo that result in a wider spectrum of mutation fixation. Indeed, these additional processes might not only be lacking in Ramos but may also be lacking in frog and shark (Diaz and

Flajnik, 1998), as well as in the 18-81 pre-B cell line (Bachl and Wabl, 1996), where immunoglobulin gene mutation has been shown to reveal a marked G/C bias (Wilson et al., 1992; Hsu, 1998).

The idea of mutation fixation being a multistage process has also emanated from a study of the strand-specificity of hypermutation (Milstein et al., 1998) as well as from an analysis of IgH mutations in mismatch repair–deficient mice. Thus, we and others have noted that a G/C-biased form of hypermutation is exhibited by mice that are deficient in Msh2 (Frey et al., 1998; Jacobs et al., 1998; Phung et al., 1998; Rada et al., 1998). This observation led Phung et al. (1998) to propose that an Msh2-dependent repair process acts to preferentially revert many of the mutations initially introduced at G/C residues, whereas we suggested the alternative possibility that Msh2 is needed to recruit a second (non-G/C-biased) stage of mutation creation (Rada et al., 1998). The G/C-biased pattern of mutation in Ramos could similarly be due to its lacking a component of the mismatch repair system that would enable it to preferentially back-repair some of the G/C-targeted mutations (although we have not detected an Msh2 defect in this line) or it could equally be that Ramos does not perform the second (A-biased phase) of mutation creation that we have envisioned.

DNA Strand Breaks Accompany Hypermutation

Most models of hypermutation envisage a role for a DNA polymerase; function of such a polymerase likely involves a breaking of the DNA backbone. We exploited the ability of TdT to add nontemplated nucleotides to the free 3′-ends of DNA to test whether breaks occurred within the V_H locus of Ramos, presuming that such nucleotide insertions (if resolved) would likely lead to the creation of IgM-loss variants. Indeed, frameshifts attributable to apparently nontemplated insertions made a large contribution to the creation of IgM-loss variants in three independent TdT transfectants; such insertions were not detected in controls. Thus, TdT-accessible sites appear to be scattered over the V_H segment but were not detected in Cμ. With regard to distribution within V_H, a larger database will be needed to determine whether the insertion sites are random, although from current data we note that two-thirds of the sites are within or directly abut the mutational hotspot consensus RGYW.

The existence of these TdT-accessible sites reveals that DNA strand breaks within the mutation domain accompany hypermutation in Ramos. DNA breaks could promote hypermutation by providing a focus for initiating error-prone DNA synthesis. Indeed, comparison of different V gene diversification strategies has prompted others to speculate that a single-/double-strand break in the V gene could initiate diversification by gene conversion in some species but by hypermutation in others (Maizels, 1995; Weill and Reynaud, 1996; Kong et al., 1998). Our data support such proposals. The only in vivo activity so far ascribed to TdT is the addition of nucleotides to the double-strand breaks created during V-(D)-J joining, but this does not allow us to exclude the possibility that the TdT insertions we observe in the Ramos transfectants have been initiated at single-strand breaks. Clearly, it will be interesting to ascertain whether hypermutation is affected by disruptions of genes involved in double-strand break repair.

At present, we cannot be sure that the breaks detected are necessary intermediates in, rather than by-products of, the hypermutation process. In any case, the existence of hypermutation-associated strand breaks could account for some of the recombination events described between immunoglobulin transgenes and the endogenous loci (Giusti et al., 1992; Winter and Gearhart, 1998). Furthermore, we note that Goosens et al. (1998) have postulated that some of the chromosomal translocations characteristic of several lymphoid neoplasms might have arisen as a by-product of the somatic hypermutation process. The demonstration that DNA strand breaks accompany V_H hypermutation in the Ramos Burkitt lymphoma line provides good support for this proposal.

Experimental Procedures

Cell Culture and Analysis

The Burkitt lines BL2, BL41, and BL70 were kindly provided by G. Lenoir (IARC, Lyon, France), and Ramos (Klein et al., 1975) was provided by D. Fearon (Cambridge, UK).

Cells were maintained in RPMI/10% FBS at 0.2–1 × 10^6/ml. Transfection of Ramos with a pSV2neo-based plasmid containing a human TdT cDNA expressed under control of the β-globin promoter and IgH enhancer (gift of M. Ehrenstein) was performed by electroporation followed by selection in medium containing G418 (4 mg/ml; GIBCO). TdT expression in nuclear extracts was monitored using a monoclonal mouse anti-human TdT (Dako). Staining for IgM was performed using FITC-conjugated goat anti-human μ (Sigma) with cell fractionation carried out on a MoFlo sorter (Cytomation).

Analysis of V Gene Diversity

Amplification of rearranged V_H segments was accomplished using Pfu polymerase together with one of 14 primers designed for each of the major human V_H families (kind gift of Ian Tomlinson; Tomlinson, 1997) and a consensus J_H back primer that anneals to all six human J_H segments (JOL48, 5′-GCGGTACCTGAGGAGACGGTGACC-3′, gift of C. Jolly). Amplification of the Ramos V_H from genomic DNA was performed with oligonucleotides RV_HFOR (5′-CCCCAAGCTTCC CAGGTGCAGCTACAGCAG) and JOL48. Amplification of the expressed V_H-Cμ cDNA was performed using RV_HFOR and Cμ2BACK (5′-CCCCGGTACCAGATGAGCTTGGACTTGCGG). The genomic Cμ1/2 region was amplified using Cμ2BACK with Cμ1FOR (5′-CCCC AAGCTTCGGGAGTGCATCCGCCCCAACCCTT); the functional Cμ allele of Ramos contains a C at nucleotide 8 of Cμ2 as opposed to T on the nonfunctional allele. Rearranged Vλs were amplified using 5′-CCCCAAGCTTCCCAGTCTGCCCTGACTCAG and 5′-CCCCTC TAGACCACCTAGGACGGTCAGCTT. PCR products were purified using QIAquick (Qiagen) spin columns and sequenced using an ABI377 sequencer following cloning into M13. Mutations were computed using the GAP4 alignment program (Bonfield et al., 1995).

For analysis of V_H gene diversification using a MutS-based assay, the Ramos V_H was PCR amplified and purified as described above using oligonucleotides containing a biotinylated base at the 5′-end. Following denaturation/renaturation (99°C for 3 min and 75°C for 90 min), the extent of mutation was assessed by monitoring the binding of the heteroduplexed material to filter-bound MutS protein with detection by ECL as previously described (Jolly et al., 1997).

Acknowledgments

We thank César Milstein and Chris Jolly for stimulating discussions and Michael Ehrenstein for advice and generous provision of the

TdT-expression plasmid. We are also indebted to Andy Riddell for cell sorting and K. J. Patel and Alex Betz for helpful suggestions.

Received September 8, 1998; revised November 4, 1998.

References

Adetugbo, K., Milstein, C., and Secher, D.S. (1977). Molecular analysis of spontaneous somatic mutants. Nature *265*, 299–304.

Alt, F.W., and Baltimore, D. (1982). Joining of immunoglobulin heavy chain gene segments: implications from a chromosome with evidence of three D-J_H fusions. Proc. Natl. Acad. Sci. USA *79*, 4118–4122.

Bachl, J., and Wabl, M. (1996). An immunoglobulin mutator that targets G.C base pairs. Proc. Natl. Acad. Sci. USA *93*, 851–855.

Bahler, D.W., and Levy, R. (1992). Clonal evolution of a follicular lymphoma: evidence for antigen selection. Proc. Natl. Acad. Sci. USA *89*, 6770–6774.

Berek, C., and Milstein, C. (1988). The dynamic nature of the antibody repertoire. Immunol. Rev. *105*, 5–26.

Betz, A.G., Neuberger, M.S., and Milstein, C. (1993). Discriminating intrinsic and antigen-selected mutational hotspots in immunoglobulin V genes. Immunol. Today *14*, 405–411.

Bonfield, J.K., Smith, K.F., and Staden, R. (1995). A new DNA-sequence assembly program. Nucleic Acids Res. *23*, 4992–4999.

Braeuninger, A., Küppers, R., Strickler, J.G., Wacker, H.-H., Rajewsky, K., and Hansmann, M.-L. (1997). Hodgkin and Reed-Sternberg cells in lymphocyte predominant disease represent clonal populations of germinal center-derived tumor B cells. Proc. Natl. Acad. Sci. USA *94*, 9337–9342.

Brüggemann, M., Radbruch, A., and Rajewsky, K. (1982). Immunoglobulin V region variants in hybridoma cells. I. Isolation of a variant with altered idiotypic and antigen binding specificity. EMBO J. *1*, 629–634.

Capizzi, R.L., and Jameson, J.W. (1973). A table for the estimation of the spontaneous mutation rate of cells in culture. Mutat. Res. *17*, 147–148.

Chapman, C.J., Mockridge, C.I., Rowe, M., Rickinson, A.B., and Stevenson, F.K. (1995). Analysis of V_H genes used by neoplastic B cells in endemic Burkitt's lymphoma shows somatic hypermutation and intraclonal heterogeneity. Blood *85*, 2176–2181.

Chapman, C.J., Zhou, J.X., Gregory, C., Rickinson, A.B., and Stevenson, F.K. (1996). V_H and VL gene analysis in sporadic Burkitt's lymphoma shows somatic hypermutation, intraclonal heterogeneity and a role for antigen selection. Blood *88*, 3562–3568.

Chui, Y.-L., Lozano, F., Jarvis, J.M., Pannell, R., and Milstein, C. (1995). A reporter gene to analyse the hypermutation of immunoglobulin genes. J. Mol. Biol. *249*, 555–563.

Clark, J.M. (1988). Novel non-templated nucleotide addition reactions catalysed by the procaryotic and eucaryotic DNA polymerases. Nucleic Acids Res. *16*, 9667–9686.

Coffino, P., and Scharff, M.D. (1971). Rate of somatic mutation in immunoglobulin production by mouse myeloma cells. Proc. Natl. Acad. Sci. USA *68*, 219–223.

Denépoux, S., Razanajaona, D., Blanchard, D., Meffre, G., Capra, J.D., Banchereau, J., and Lebecque, S. (1997). Induction of somatic mutation in a human B cell line in vitro. Immunity *6*, 35–46.

Diaz, M., and Flajnik, M.F. (1998). Evolution of somatic hypermutation and gene conversion in adaptive immunity. Immunol. Rev. *162*, 13–24.

Frey, S., Bertocci, B., Delbos, F., Quint, L., Weill, J.-C., and Reynaud, C.-A. (1998) Mismatch repair deficiency interferes with the accumulation of mutations in chronically stimulated B cells and not with the hypermutation process. Immunity *9*, 127–134.

Giusti, A., Coffee, R., and Manser, T. (1992). Somatic recombination of heavy chain V region transgenes with the endogenous heavy chain locus in mice. Proc. Natl. Acad. Sci. USA *89*, 10321–10325.

Goossens, T., Klein, U., and Küppers, R. (1998). Frequent occurrence of deletions and duplications during somatic hypermutation: implications for oncogenic translocations and heavy chain disease. Proc. Natl. Acad. Sci. USA *95*, 2463–2468.

Green, N.S., Lin, M.M., and Scharff, M.D. (1998). Immunoglobulin hypermutation in cultured cells. Immunol. Rev. *162*, 77–87.

Hsu, E. (1998). Mutation, selection and memory in B lymphocytes of exothermic vertebrates. Immunol. Rev. *162*, 25–36.

Jacobs, H., Fukita, Y., van der Horst, G., de Boer, J., Weeda, G., Essers, J., de Wind, N., Endelward, B.P., Samson, L., Verbeek, S., et al. (1998). Hypermutation of immunoglobulin genes in memory B cells of DNA repair-deficient mice. J. Exp. Med. *187*, 1735–1743.

Jain, R., Roncella, S., Hashimoto, S., Carbone, A., Franco di Celle, P., Foa, R., Ferrarini, M., and Chiorazzi, N. (1994). A potential role for antigen selection in the clonal evolution of Burkitt's lymphoma. J. Immunol. *153*, 45–52.

Jolly, C.J., Wagner, S.D., Rada, C.A., Klix, N., Milstein, C., and Neuberger, M.S. (1996). The targeting of somatic hypermutation. Semin. Immunol. *8*, 159–168.

Jolly, C.J., Klix, N., and Neuberger, M.S. (1997). Rapid methods for the analysis of immunoglobulin gene hypermutation: application to transgenic and gene targeted mice. Nucleic Acids Res. *25*, 1913–1919.

Kim, S., Davis, M., Sinn, E., Patten, P., and Hood, L. (1981). Antibody diversity: somatic hypermutation of rearranged VH genes. Cell *27*, 573–581.

Klein, G., Giovanella, B., Westman, A., Stehlin, J., and Mumford, D. (1975). An EBV negative cell line established from a American Burkitt lymphoma; receptor characteristics, EBV infectability and permanent conversion into EBV-positive sublines by in vitro infection. Intervirology *5*, 319–334.

Kong, Q., Harris, R.S., and Maizels, N. (1998). Recombination based mechanisms for somatic hypermutation. Immunol. Rev. *162*, 67–76.

Kosmas, C., Viniou, N-A., Stamatopoulos, K., Courtenay-Luck, N.S., Papadaki, T., Kollia, P., Paterakis, G., Anagnostiou, D., Yataganas, X., and Loukopoulos, D. (1996). Analysis of the κ light chain variable region in multiple myeloma. Brit. J. Haematol. *94*, 306–317.

Lo, A.K., Ching, A.K., Lim, P.L., and Chui, Y.L. (1997). Strand breaks in immunoglobulin gene hypermutation. Ann. NY Acad. Sci. *815*, 432–435.

Luria, S.E., and Delbrück, M. (1943). Mutations of bacteria from virus sensitivity to virus resistance. Genetics *28*, 491–511.

Maizels, N. (1995). Somatic hypermutation: how many mechanisms diversify V region sequences? Cell *83*, 9–12.

McKean, D., Huppi, K., Bell, M., Staudt, L., Gerhard, W., and Weigert, M. (1984). Generation of antibody diversity in the immune response of BALB/c mice to influenza virus haemagglutinin. Proc. Natl. Acad. Sci. USA *81*, 3180–3184.

Milstein, C., Neuberger, M.S., and Staden, R. (1998). Both strands of antibody genes are hypermutation targets. Proc. Natl. Acad. Sci. USA *95*, 8791–9784.

Neuberger, M.S., and Milstein, C. (1995). Somatic hypermutation. Curr. Opin. Immunol. *7*, 248–254.

Parham, P. (1998). Somatic hypermutation of immunoglobulin genes. Immunol. Rev. *162* (Copenhagen, Denmark: Munksgaard).

Phillips, J.W., and Morgan, J.W. (1994). Illegitimate recombination induced by DNA double-strand breaks in a mammalian chromosome. Mol. Cell. Biol. *14*, 5794–5803.

Phung, Q.H., Winter, D.B., Cranston, A., Tarone, R.E., Bohr, V.A., Fishel, R., and Gearhart, P.J. (1998). Increased hypermutation at G and C nucleotides in immunoglobulin variable genes from mice deficient in the MSH2 mismatch repair protein. J. Exp. Med. *187*, 1745–1751.

Rada, C.A., Ehrenstein, M.R., Neuberger, M.S., and Milstein, C. (1998). Somatic hypermutation in MSH2 deficient mice is more focussed on intrinsic hotspots suggesting targeting to be a two stage process. Immunity *9*, 135–141.

Ratech, H. (1992). Rapid cloning of rearranged immunoglobulin heavy chain genes from human B-cell lines using anchored polymerase chain reaction. Biochem. Biophys. Res. Commun. *182*, 1260–1263.

Reynaud, C.-A., and Weill, J.-C. (1996). Somatic hypermutation: mechanisms and signals. Semin. Immunol. *8*, 125–184.

Rogozin, I.B., and Kolchanov, N.A. (1992). Somatic hypermutation of immunoglobulin genes. II. Influence of neighbouring base sequences on mutagenesis. Biochem. Biophys. Acta *1171*, 11–18.

Tomlinson, I.M. (1997). V Base database of human antibody genes. Medical Research Council, Centre for Protein Engineering, UK. http://www.mrc-cpe.cam.ac.uk/.

Wabl, M., Burrows, P.D., von Gabain, A., and Steinberg, C.M. (1985). Hypermutation at the immunoglobulin heavy chain locus in a pre-B-cell line. Proc. Natl. Acad. Sci. USA *82*, 479–482.

Wagner, S.D., Milstein, C., and Neuberger, M.S. (1995). Codon bias targets mutation. Nature *376*, 732.

Wagner, S.D., Elvin, J.G., Norris, P., McGregor, J.M., and Neuberger, M.S. (1996). Somatic hypermutation of Ig genes in patients with xeroderma-pigmentosum (XP-D). Int. Immunol. *8*, 701–705.

Weill, J.-C., and Reynaud, C.-A. (1996). Rearrangement/hypermutation/gene conversion: when, where and why? Immunol. Today *17*, 92–97.

Wilson, M., Hsu, E., Marcuz, A., Courtet, M., Du Pasquier, L., and Steinberg, C. (1992). What limits affinity maturation of antibodies in Xenopus, the rate of somatic mutations or the ability to select mutants? EMBO J. *11*, 4337–4347.

Wilson, P.C., de Boutellier, O., Liu, Y-J., Potter, K., Banchereau, J., Capra, J.D., and Pascual, V. (1998). Somatic hypermutation introduces insertions and deletions into immunoglobulin V genes. J. Exp. Med. *187*, 59–70.

Winter, D.B., and Gearhart, P.J. (1998). Dual enigma of somatic hypermutation of immunoglobulin variable genes; targeting and mechanism. Immunol. Rev. *162*, 89–96.

Wu, H.Y., and Kaartinen, M. (1995). The somatic hypermutation activity of a follicular lymphoma links to large insertions and deletions of immunoglobulin genes. Scand. J. Immunol. *42*, 52–59.

Wu, H.Y., Pelkonen, E., Knuutila, S., and Kaartinen, M. (1995). A human follicular lymphoma B cell line hypermutates its functional immunoglobulin genes in vitro. Eur. J. Immunol. *25*, 3263–3269.

Zheng, B., Han, S., Spanopoulou, E., and Kelsoe, G. (1998). Immunoglobulin gene hypermutation in germinal centres is independent of the RAG-1 V(D)J recombinase. Immunol. Rev. *162*, 133–141.

Zhu, M., Rabinowitz, J.L., Green, N.S., Kobrin, B.J., and Scharff, M.D. (1995). A well-differentiated B cell line is permissive for somatic mutation of a transfected immunoglobulin heavy-chain gene. Proc. Natl. Acad. Sci. USA *92*, 2810–2814.